The 2009 IEEE/RSJ International Conference on
Intelligent Robots and Systems
October 11-15, 2009 St. Louis, USA

Towards On-line Fingertip Bio-impedance Identification for Enhancement of Electro-tactile Rendering

John Gregory and Ning Xi
Dept. of Electrical and Computer Engineering
Michigan State University
East Lansing, MI 48824
{gregor87, xin}@egr.msu.edu

Yantao Shen
Dept. of Electrical and Biomedical Engineering
University of Nevada-Reno
Reno, Nevada 89557-0260
ytshen@unr.edu

***Abstract*— Research in rehabilitation engineering shows that electrodes can produce tactile sensations with appropriate electrical signals tailored to stimulate the multiple tactile receptors located under the fingertip skin. However, electrical stimulation that is suitable in terms of current or voltage level for tactile sensations experienced from an individual cannot be guaranteed for every user; the dynamic range is largely dependent on the user. An identification method is then necessary for characterizing the parameters of the skin-electrode interface circuit model as to improve rendering consistency and comfort for every user regardless of skin condition. In this paper, we focus on developing a custom-built electro-tactile display terminal for data collection and an identification method to determine the individual bio-impedance parameters based on the well-known skin-electrode interface circuit model: the Cole-Cole circuit model. The goal of this work is to develop an on-line identification and stimulation current control approach for enhancement of electro-tactile-based rendering in applications such as rehabilitation, sensory substitution, telepresence, etc.**

***Index Terms*— Electro-tactile Rendering Display, Fingertip, Skin-electrode Interface, Bio-impedance, Identification**

I. INTRODUCTION

Electrodes designed to substitute touch sensation have been performed on various locations on the body. The tongue [14], the abdomen [11], and fingertip [8]-[10] are areas most studied to assess the ability of human subjects to detect and identify patterns using these devices. This research has shown that electrical stimuli can deliver a significant amount of information about patterns of stimuli; thus, ample research supports the notion that electrical stimuli are a viable means for delivering sensory information.

Our research interest pertains to the investigation of the ability to induce touch sensations on the fingertip skin using an electrical array. This mechanism, also called electro-tactile or electro-cutaneous stimulation, is illustrated in Figure 1. The fingertip skin consists of several horizontal layers: seven classes of mechanoreceptors, two classes of thermoreceptors, four classes of nociceptors, and three classes of proprioceptors are found within these layers of the skin. Several research findings in the areas of psychophysics, neurocytology, electrochemistry, and cognitive science have shown that mechanical or electrical stimulations to these receptors produce tactile feelings in humans [6][16]. Inspired by these explorations, electro-tactile research and development have been forming the potential to advance assistive, diagnostic, and rehabilitative devices such as Braille readers, sensory substitution, teleoperation and telepresence, and computer games [2][8][10].

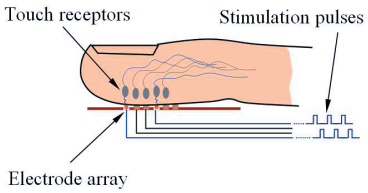

Fig. 1. Illsutration of fingertip electro-tactile through electrode arrays.

Currently, although such electro-tactile display technology has been extensively conducted, electro-tactile stimulation can be uncomfortable because of the highly variable conditions at the electrode-skin interface. The quality control of tactile sensation/preference through the electrode-skin interface is still an open research problem [4][8][10][14].

In this paper, we focus on developing an initial identification method to extract user bio-impedance parameters for electro-tactile calibration. The goal of our work is to identify the parameters on-line and to use them to automatically tune the voltage/current to a desired sensation level for each user. The work will provide an effective solution to user-friendly, electro-tactile technology for rehabilitation, sensory substitution, and telepresence applications.

This paper is structured as follows: The custom-built electro-tactile display system and output waveforms are described in Section II. Skin electrical properties and skin-electrode interface models are reviewed in Section III. Based on the equivalent Cole-Cole skin-electrode circuit model, the proposed bio-impedance identification methods are introduced in Section IV. In Section V, the experimental validation and the identification results are demonstrated and analyzed. Finally, we conclude the work in Section VI.

II. DEVELOPMENT OF ELECTRO-TACTILE DISPLAY SYSTEM

A. Electrode Array of Electro-tactile Display

The developed electro-tactile display is an electrode array device that evokes tactile (touch) sensations within the fin-

This research work is partially supported under U.S. Army Contract No. W56HZV-04-2-001, U.S. Army Research Office Contract No. W911NF-07-D-001, and the Nevada System of Higher Education IBRAF grant (NSHE-09-X27).

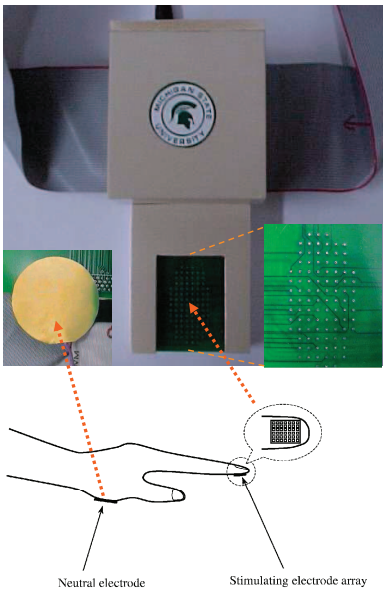

Fig. 2. Electro-tactile display terminal and electrode arrangement.

gertip skin by passing a local electric current through the skin to stimulate afferent nerve fibers or receptors via the electrodes placed against the skin surface. To ensure safety, a protective circuit is included in the display.

Electro-tactile stimulation needs both stimulating electrodes and a neutral electrode return. In our design, the small electrode array is used as the stimulating electrode array. The stimulating electrode array is shown in Figure 2. In the figure, the array for the fingertip (index) has 98 stimulation electrodes within an area measuring 25×12 mm^2. Each electrode area is 0.454 mm^2 with a density of 32 electrodes per cm^2 and 2 mm pitch. These values are roughly consistent with reported spatial resolution of the relevant tactile receptors at the fingertips [4][9][10]. The electrode array board is custom-manufactured PCB. The designed fingertip-shaped cross section of the display terminal helps conform to the index fingertip. Another large electrode (706.5 mm^2) is used as the neutral electrode and is located in the thenar area close to the thumb. According to the arrangement of the electrodes, the stimulating current will pass through the fingertip skin at multiple locations of the electrode array and then move to the neutral electrode (like ground) through the tissues between the fingertip and the thenar. Figure 2 also shows the arrangement of the two electrode pieces in the developed electro-tactile display terminal.

B. Driver Circuitry of Electro-tactile Display

A popular design of circuit topologies set the direct-current (DC) magnitudes of current drivers to stimulate mechanoreceptors. This assumes that the stimulation level and sensation is independent of the fingertip load impedance if the equivalent fingertip load is much smaller in magnitude than the driver impedance. Conversely, setting the voltage output as a way of providing the stimulation heavily depends on each user's skin condition. Our approach is based on the

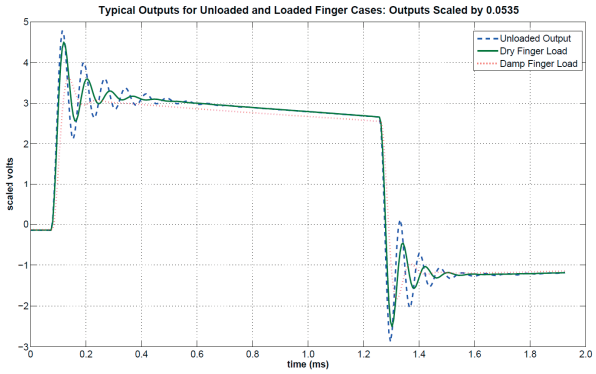

Fig. 3. Typical terminal output waveforms with dry and damp fingertip loads and no load, scaled by 0.0535.

latter using step up transformers and switching logic to drive the electrode array. In practice, the benefits of our approach afford ease of design because of the in-series small circuit impedance compared to the high human load impedance, unneeded high voltage supplies, and natural ground isolation at the output stage of the transformer drivers; however, it will require real-time digital control of the output current amplitude for user comfort. In contrast, constant current drivers require intricate design related to the usually high human DC electrical resistance and high voltage supply hookups needed to drive the current-controlled opAmps but are not influenced dramatically by changes in skin impedance. There drawback comes from power inefficiency w.r.t. large loads as discussed in [3]. The numerical limits of quasi-static DC resistance for dry skin range as large as 1 to 100 $M\Omega$ and as low as 10 $K\Omega$ when normalized to a 1 mm^2 electrode area [2][3][4]. It should be noted that these values heavily dependent on injected current amplitudes. Additionally, the voltage at the terminal output must usually be high (100-400 volts) for our stimulation current levels (less than 5 mA) and at our electrode dimensions.

C. Display Terminal Output Waveforms

The typical outputs of both the unloaded (no fingertip skin engaged) and loaded (during dry or damp fingertip skin engagement) terminals of the developed electro-tactile display are the voltages generates from square-waves, as shown in Figure 3. From this, the seen challenges with our design include: 1) the significant transient response at the front and tail of the waveform due to large inductive and capacitive effects from the step-up transformers; 2) voltage droop at steady state due to resistivity in the transformer wires; Both of these can be compensated for by identifying the circuit model and employing closed-loop control law.

III. SKIN-ELECTRODE CIRCUIT MODELS

A. Circuit Model and Parameters

The task of transcutaneous electrical stimulation is to overcome the impedance of the skin to activate the receptor or sensory nerves underlying the surface [1]. The surface electrodes problem can be presented by an equivalent circuit

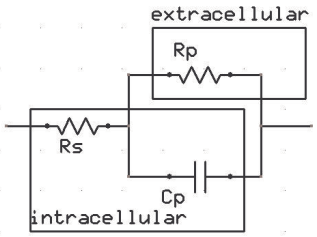

Fig. 4. Cole-Cole based interface model for small stimulation currents less than about 5 mA.

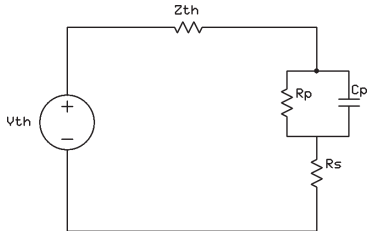

Fig. 5. V_{th} is the unloaded measured output. Z_{th} represents the 5th order equivalent impedance of the step-up transformer. The output under RC load is the 1st order bio-impedance model

of the electrodes and its interface with the skin. Under the surface electrodes, characterizing the skin resistance and capacitance should allow for an accurate equivalent circuit model for human skin. The simplest, yet effective, equivalent circuit model that can be used to represent skin impedance is a parallel network consisting of a capacitor and resistor, followed by a series resistor [1][3][4]. Broadly, the parallel capacitor and resistor, C_p and R_p, in this model represent the electrical properties of the upper stratum corneum (SC), and the series resistor, R_s, represents the impedance of the subdermal medium. The more complete model would consider the skin as composed of numerous layers of cells, each having capacitance and conductance [1][3][4][6][15].

B. Selected Skin-Electrode Interface Model for Identification

Our parameter identification of the skin bio-impedance model is shown in Figure 4. For an in-depth discussion of this representation, please see [6]. We assume small stimulation currents in the low to sub-milliamp regime that suffice the model and allow us to ignore nonlinearities associated with increased current. [1][3][4]. Here, R_p represents extracellular compartments in the stratum corneum (SC) such as pores and pathways through the laminar bilayers [5]. C_p models the hydrophobic lipid membranes and laminar bilayer composition that separate extracellular and intracellular corneocyte components. R_s represents the intracellular pathways through the corneocytes and underlying bulk tissue resistivity and dominates as frequency become high (see [12] for physical structure). As mentioned R_p, is usually the largest resistive element (20 $K\Omega$ to 1 $M\Omega$). Typical ranges of C_p are on the nanofarad to sub-nanofarad order (normalized to our electrode dimensions) [2][3][4]. As well, R_s is low in the kilo- to sub kilo-Ohm range [1][4][5].

IV. IDENTIFICATION METHODOLOGY

The focus of this section presents an identification method that calculates the parameters of the finger bio-impedance and driver circuit thevenin impedance Z_{th} by sampling the loaded and unloaded state of the output based on the circuit shown in Figure 5. Here, V_{th} is taken as the new input to the system and is equivalent to the unloaded output condition. It is assumed that the original input for the transformers are square wave pulses with programmed amplitude, pulse frequency and duty cycle values of 4.2 Volts, 60 Hertz and 4 percent, respectively. This produces approximately a 50 Volt pulse at the output of the display. We keep the stimulating voltage low as not to startle the subjects on which we test the device.

A. Data Acquisition for identification

The process starts by sampling the unloaded output of the system with a data acquisition board (DAQ). For off-line identification, this is done once during the calibration process as the circuit model is assumed LTI. The sampled output under load consists of known resistor values or a human index fingertip to identify either Z_{th} or bio-impedance parameters, respectively. We use a buffered voltage measurement circuit to scale down the large output voltage amplitude to meet the dynamic range of the DAQ (0.0535 scale factor).

B. Identification Algorithm

The identification algorithm modifies the established Kalman successive iteration least-squares [7]. The algorithm first minimizes the output error energy cost function for i=0:

$$E = \oint \left| X\frac{N_i}{D_{i-1}} - W\frac{D_i}{D_{i-1}} \right|^2 \frac{dz}{z} = \oint \left| X\frac{N_i}{D_i} - W \right|^2 \frac{D_i^2}{D_{i-1}^2}\frac{dz}{z} \quad (1)$$

for i = 1, 2, 3, $\cdots$, and D_{-1}=D_0=1,

of the finite impulse response (FIR) system illustrated in Figure 6. Note that **X** and **W** are the respective measured input and output records, and **N** and **D** consist of the unknown one-port rational function numerator and denominator parameters, α and β, respectively, of an assumed order that we wish to identify. This system is iterative and pre-filters the input and output record using the a priori identified denominator to solve the a posteriori set of model parameters for $D_0 \geq 1$. The initial global minimum gradient solution to Eqn. (1) for i=0 is:

$$\delta = \mathbf{Q}^{-1}\mathbf{c} = \begin{pmatrix} \alpha \\ -\beta \end{pmatrix}. \quad (2)$$

Q and **c** are the correlation matrix and parameter vector, respectively. The minimized output error energy converges to the error between the IIR rational model and measured outputs asymptotically if the denominator quotient in Eqn. (1) converges.

For each iteration, we compare the measured to the predicted output by using root relative square error goodness-of-fit criteria (RRSE):

$$RRSE_i = \sqrt{\frac{(V_i - W)\bullet(V_i - W)}{(W - W_\mu)\bullet(W - W_\mu)}}, \quad (3)$$

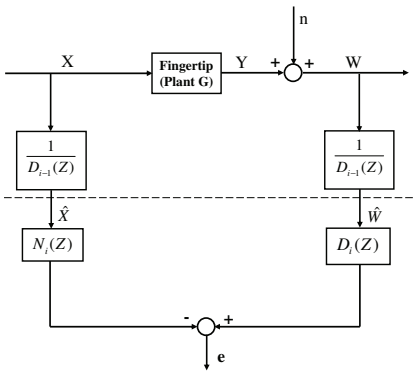

Fig. 6. The iterative pre-filtering scheme for identification.

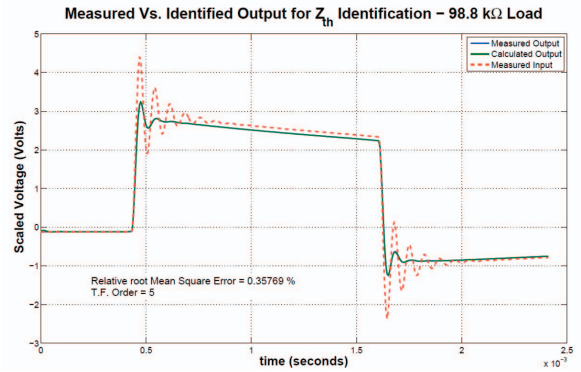

Fig. 7. Identified Z_{th} using a 98.8 $K\Omega$ reference load. Output is scaled by 0.0535.

where $\mathbf{V}$ is the predicted output vector, $\mathbf{W}$ the measured output vector, and $\mathbf{W}_\mu$ the mean of the measured output for a given iteration. We chose this metric so that linear signal scaling would not influence comparison of error magnitudes.

V. EXPERIMENTAL VALIDATION AND RESULTS EVALUATION

A. Offline Identification of Driver Circuit Z_{th}

We test the described algorithm by identifying the parameters of a 5th order model of the step-up transformers' thevenin impedance Z_{th}:

$$Z_{th} = \frac{\alpha_0 + \alpha_1 z^{-1} + \cdots + \alpha_4 z^{-(4)}}{1 + \beta_1 z^{-1} + \cdots + \beta_5 z^{-5}}, \tag{4}$$

where the parameters α_i and β_i are defined in Eqn. (2). The system order is based on the non-ideal transformer model in [13]. The output V_{out} is measured using a known load value of $R_L = 98.8K\Omega$. Using this data, the algorithm solved the impedance parameters based on the relation:

$$N_{th_i} V_{out} = D_{th_i}[R_L(V_{th} - V_{out})]. \tag{5}$$

Where

$$X = V_{out} \quad and \quad W = [R_L(V_{th} - V_{out})], \tag{6}$$

are the modified input and output records. N_{th_i} and D_{th_i} represent the i_{th} estimation of the Z_{th} numerator and denominator, respectively. Figure 7 compares a trial of the measured and predicted output under the known R_L in Eqn. (5) using the identified Z_{th}. The RRSE gives a good result of less than 1%.

To test the prediction validity of the identified Z_{th} one-port in Eqn. (4), we predicted the outputs of the identified system model and compared them to measured outputs of known resistive loads via a rearrangement of Eqn. (5). Resistor values of R_{actual} = 21.62, 55.20, 216.6, 328.9, and 555.0 $K\Omega$ were each attached and the outputs sampled to fit a 1st order Z_L model to each. The values of the resistors realize a range of the reported values of human DC skin resistances for various skin conditions at our electrode dimensions and were selected for this reason [2]. The 216.8 $K\Omega$ model-predicted time-response versus the measured output presented in Table I summarizes the results of measured load, predicted load, RRSE (predicted vs. measured output voltage waveform) and measurement error in DC resistance. The values give acceptable accuracy for our purpose and may improve with a greater number of sampled periods in the data set.

TABLE I
VALIDITY TESTS OF IDENTIFICATION ALGORITHM FOR A KNOWN LOAD

Measured R	Predicted R	RRSE	Error % of Acc. vs. Ident.
21.62 $K\Omega$	20.70 $K\Omega$	13.45%	4.26%
55.20 $K\Omega$	55.43 $K\Omega$	4.31%	0.42%
216.6 $K\Omega$	237.4 $K\Omega$	0.99%	9.60%
328.9 $K\Omega$	368.9 $K\Omega$	8.65%	12.2%
555.0 $K\Omega$	556.4 $K\Omega$	4.31%	0.25%

B. Identification of Fingertip Skin Bio-Impedance

We relied on the Cole-Cole 1st order bio-impedance model Z_{bio} presented in subsection B of section III (refer to Figure 4). The human model in the s-domain is:

$$Z_{bio}(s) = \frac{(R_s + R_p) + R_s R_p C_p s}{1 + R_p C_p s}. \tag{7}$$

From the driver and load model circuit, we derive the following relation:

$$D_{bio_i}[Z_{th} V_{out}] = N_{bio_i}[V_{th} - V_{out}], \tag{8}$$

where Z_{th} is the identified driver circuit impedance described in Eqn. (4), and N_{bio_i} and D_{bio_i} constitute the numerator and denominator of Z_{bio}, respectively. The reformulated input and output vectors in Eqn. (1) are now:

$$X = V_{th} - V_{out} \quad and \quad W = Z_{th} V_{out}. \tag{9}$$

Then, using the asymptotic value Z_{bio_∞} and Eqn. (7), the program calculates the parameters of the user's RC-modeled bio-impedance:

$$Z_{bio_\infty}\left(\frac{1}{C_p R_p} = s_c\right) = \frac{(2R_s + R_p)}{\sqrt{2}} \tag{10}$$

$$R_s = Z_{bio_\infty}(\infty) \tag{11}$$

$$R_p = Z_{bio_\infty}(0) - R_s \tag{12}$$

We identified 20 RC models based on Eqn. (7) under a dry index fingertip load for one subject to test the method's

repeatability. An additional 12 models were produced under wetted fingertip measurements. For latter case, the subject placed his finger in untreated tap water and briefly rubbed it in to the skin. This process is an attempt at mimicking the ion solute found in sweat production. Figure 8 (a) and (b) show one of 20 results under a dry index and, similarly, Figure 9 (a) and (b) for the damp fingertip case. Corresponding to the above experiments under both conditions, Tables II and III give the mean $\bar{X}$ and standard deviation s of each of the calculated values in Eqns. (11∼13) along with the calculated low pass corner frequency f_c and RRSE. R_s has the largest variance. This may be a consequence of its reduced role w.r.t. influencing the output transients and that $R_p \gg R_s$ in Eqn. (7). As such, the small R_sC_p product locates the zero of the load network at a much higher frequency than the bio-impedance pole location; hence, R_s is more susceptible to measurement noise and model error. Conversely, R_p mainly determines the pole location and subtly influences the zero due to its larger magnitude. This value then heavily determines the shape of the loaded output and should vary the least, as is seen. C_p influences both the pole and zero location heavily and shows a variance intermediate of R_p and R_s as expected.

Furthermore, we built a circuit model of the identified parameters of our subject's dry fingertip identification to determine the accuracy of the identification and validity of the proposed model, illustrated in Figure 4, by using the following procedure: investigating the RRSE and waveform shape "goodness of fit" between the circuit and the fingertip measurement output; and studying the known circuit elements against the subject's identified parameters. The values chosen to build the circuit model for this experiment are as follows: R_p = 179.8 $K\Omega$; C_p = 0.12 nF; and R_s = 32.46 $K\Omega$. These values reflect the mean identified parameters in Table II within 5% tolerance each.

Table IV summarizes the statistical results for the built RC model for all 23 identification trials. The means $\bar{X}$ of the identified circuit elements for all these identification trials agree with the magnitudes of the actual circuit elements suggesting an accurate identification method and further validates the transformer identified model. R_p varies the least, C_p intermediately, and R_s the most and is consistent with prior tests. Figure 10 graphs the measured outputs under load for both the measured dry fingertip and the measured output of the representative circuit including the unloaded waveform. From this, we conclude that the results of this test subject's bio-impedance signature against the representative circuit validates the selected Cole-Cole model for the specified operating conditions and stimulating waveform shape in that it can predict the output. As well, comparing Table II and IV suggest the the subject's identified parameters reflect at least a rudimentary physical process of the electrode-skin interface and hints at an accurate model.

Based on the effectiveness of parameter identification for bio-impedance of human fingertip skin, under the same unloaded output wave and the same scale factor 0.0535, we further conduct the identification of parameters for 10 different subjects: both male and female, ages from 26 to 40 years old. For the damp finger condition, the identified R_p is from 20.2$K\Omega$ to 165$K\Omega$, R_s varies from 3.93$K\Omega$ to 19.8$K\Omega$, and C_p varies from 160pF to 845pF. The RRSE of the identification is within 5.6%. While for the dry finger condition, the identified R_p is from 194$K\Omega$ to 616$K\Omega$, R_s varies from 19$K\Omega$ to 69.8$K\Omega$, and C_p varies from 45.4pF to 165pF. The RRSE is within 6.1%. The results show the various bio-impedance parameters corresponding to different users. The identified values are within the reasonable range previously reported [4].

TABLE II

SUMMARY STATISTICS (REF. FIGURE 4) (N = 16 I/O COMBINATIONS): ONE SUBJECT DRY INDEX FINGERTIP - MALE; 29 YEARS OLD

stat	$f_c(KHz)$	R_p $(K\Omega)$	$C_p(nF)$	R_s $(K\Omega)$	RRSE (%)
$\overline{X}$	8.33	185.96	0.12	33.40	6.38
s	3.34	55.32	0.04	15.24	1.53

TABLE III

SUMMARY STATISTICS (REF. FIGURE 4) (N = 12 I/O COMBINATIONS): ONE SUBJECT DAMP INDEX FINGERTIP - MALE; 29 YEARS OLD

stat	$f_c(KHz)$	R_p $(K\Omega)$	$C_p(nF)$	R_s $(K\Omega)$	RRSE (%)
$\overline{X}$	14.79	17.36	0.66	6.14	4.97
s	4.35	3.35	0.10	1.43	1.37

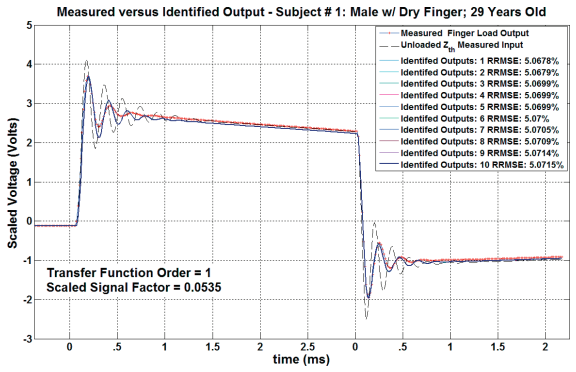

(a)

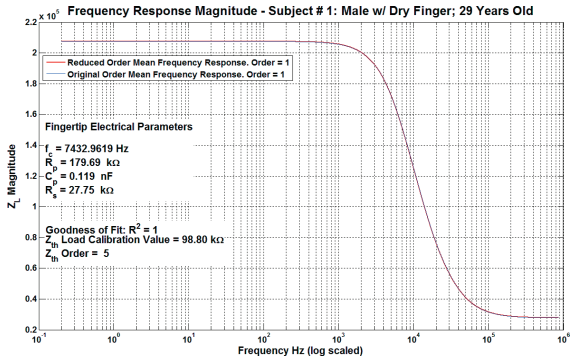

(b)

Fig. 8. (a) One of 20 voltage outputs (typical) under dry index fingertip load; (b) Frequency response and identification parameters based on (a).

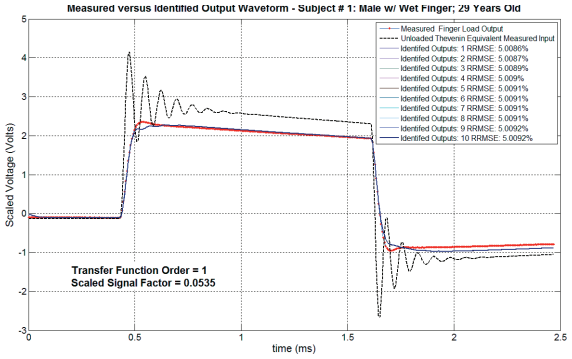

(a)

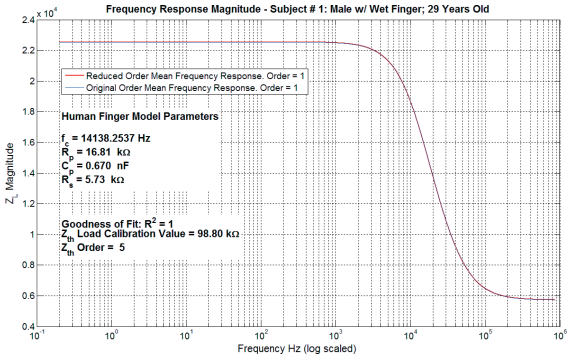

(b)

Fig. 9. (a) One of 12 voltage outputs (typical) under damp index fingertip load; (b) Frequency response and identification parameters based on (a).

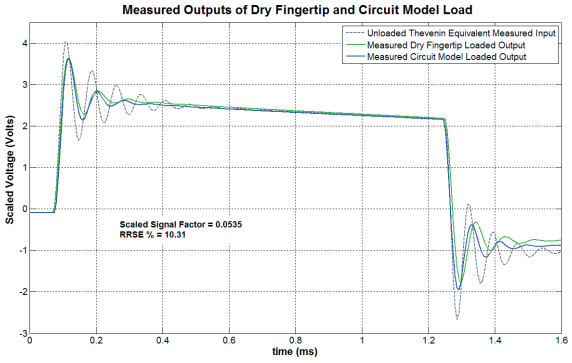

Fig. 10. Graph of measured dry fingertip and circuit model output; scaled by 0.0535; RRSE = 10.31 %

TABLE IV

SUMMARY STATISTICS (REF. FIGURE 4) (N = 23 I/O COMBINATIONS): ACTUAL VERSUS IDENTIFIED CIRCUIT ELEMENTS

Element	R_p $(K\Omega)$	$C_p(nF)$	R_s $(K\Omega)$	RRSE (%)
Actual	179.8	0.120	32.46	$***$
$\overline{X}$	184.34	0.134	27.43	6.39 %
s	32.32	0.036	11.85	2.03 %
% error	2.46 %	10.40 %	15.50 %	$***$

VI. CONCLUSIONS AND FUTURE WORK

In this paper, a fingertip skin bio-impedance identification algorithm for the enhancement of electro-tactile rendering is presented and experimentally validated. By utilizing the identified bio-impedance parameters of the employed skin-electrode circuit model (Cole-cole model), setting the stimulation current output to a comfortable dynamic range while maintaining proper stimulation levels for every user becomes possible using voltage output drivers. This implies that this work is providing an effective solution to user-friendly electro-tactile technology for applications such as rehabilitation and telepresence. In addition, the parameter identification of 10 subjects with both dry and damp skin moisture regimes was detailed in this work. The wide parameter variation between participants under constant operating conditions has suggested us to develop an adjustable control mechanism for on-line quality tuning of individual tactile preference in the future work.

REFERENCES

[1] S. J. Dorgan, "A Model for Human Skin Impedance During Surface Functional Neuromuscular Stimulation", *IEEE Transactions On Rehabilitation Engineering*, Vol. 7, No. 3, SEPT. 1999.

[2] E. F. Prokhorov, et al., "In Vivo Electrical Characteristics of Human Skin, Including at Biological Active Points", *Medical and Biological Engineering and Computing*, Vol. 38, pp. 507-511, 2000.

[3] C. J. Poletto and C. L. Van Doren, "A High Voltage, Constant Current Stimulator for Electrocutaneous Stimulation Through Small Electrodes", *IEEE Transactions On Biomedical Engineering*, Vol. 46, No. 8, pp. 929-936, 1999.

[4] K. A. Kaczmarek, J. G. Webster, et al., "Electrotactile and Vibrotactile Displays for Sensory Substitution Systems", *IEEE Transactions On Biomedical Engineering*, Vol. 38, No. 1, pp. 1-15, 1991.

[5] U. Pliquett, R. Langer, and J. C. Weaver, "Changes in the Passive Electrical Properties of Human Stratum Corneum Due to Electroporation", *Biochimica et Biophysica Acta*, Vol. 1239, pp. 111-121, 1995.

[6] K. R. Foster and H. C. Lukaski, "Whole-body Impedance–What Does It Measure?", *Am J Clin Nutr*, Vol. 64, pp. 388S-396S, 1996.

[7] K. Steiglitz and L. E. McBride, "A Technique for the Identification of Linear Systems", *IEEE Transactions on Automatic Control*, pp. 461-464, Oct 1965.

[8] A. Y. J. Szeto and R. R. Riso, "Sensory Feedback Using Electrical Stimulation of the Tactile Sense", *In R.V. Smith and J.H. Leslie, Jr. (Eds.), Rehabilitation eng.*, pp. 29-78, Boca Raton: CRC Press, 1990.

[9] L. R. Bobich, J. P. Warren, J. D. Sweeney, S. I. Helms Tillery, and M. Santello, "Spatial Localization of Electro-tactile Stimuli on the Fingertip in Humans", *Somatosensory and Motor Research*, Vol. 24, No. 4, pp. 179-188, 2007.

[10] H. Kajimoto, N. Kawakami, S. Tachi, and M. Inami, "SmartTouch: Electric Skin to Touch the Untouchable", *IEEE Computer Graphics and Applications: Emerging Tech.*, Vol. 24, No. 1, pp. 36-43, 2004.

[11] S. J. Haase, K. A. Kaczmarek, "Electrotactile Perception of Scatterplots on the Fingertips and Abdomen", *Medical Biological Engineering and Computing*, Vol 43, pp. 283-289, 2005.

[12] H. Brannon, MD, "Stratum Corneum: Top Layer of the Epidermis-Structure and Function", Accessed: Feb. 12, 2009. Available in: http://dermatology.about.com/od/anatomy/ss/sc_anatomy.htm.

[13] "Pulse Transformers", Online document. Accessed: Feb. 14, 2009. Available in: http://www.rhombus-ind.com/app-note/circuit.pdf.

[14] K. A. Kaczmarek and M. E. Tyler, "Effect of Electrode Geometry and Intensity Control Method on Comfort of Electro-tactile Stimulation on the Tongue", *Proc. of the ASME Dynamic Systems and Control Division*, Vol. 2, pp. 1239-1243, 2000.

[15] A. Boxtel, "Skin Resistance During Square-wave Electrical Pulses of 1 to 10 mA", *Medical Biological Engineering and Computing*, Vol. 15, pp. 679-687, 1977.

[16] A. B. Vallbo and R. S. Johansson, "Properties of Cutaneous Mechanoreceptors in the Human Hand Related to Touch Sensation", *Human Neurobiology*, Vol. 3, pp. 3-14, 1984.